Chem Soc Rev

Cite this: *Chem. Soc. Rev.*, 2012, **41**, 5672–5686

www.rsc.org/csr

TUTORIAL REVIEW

Quinoidal oligothiophenes: new properties behind an unconventional electronic structure

Juan Casado,* Rocío Ponce Ortiz and Juan T. López Navarrete*

Received 15th March 2012
DOI: 10.1039/c2cs35079c

The main chemical, spectroscopic and material research done in tetracyano quinoidal oligothiophenes in the last 30 years has been reviewed. Their use as semiconducting substrates in organic electronic and their versatility to act as multifunctional materials have been highlighted. This tutorial review has been paralleled by the description of the main findings provided by Raman spectroscopy, in particular, associated with the discovery of the intrinsic diradical properties inherent to the pro-aromatic character of the quinoidal arrangement. It turns out that the fascinating properties of these materials are the manifestation of the diradical fingerprint behind a rather unconventional electronic structure.

Introduction

In 2000 the Nobel Prize in Chemistry awarded the work of Shirakawa, McDiarmid and Heeger for the discovery and development of conducting polymers.[1,2] Conducting polymers are characterized by an alternating sequence of single and double bonds (conjugated polymers, Fig. 1a).[3–5] Most often these are constructed with aromatic (hetero)cyclic units giving rise to pristine conducting polymers based on aromatic monomers, such as polythiophene, polypyrrole, polyparaphenylene, polyfuran, *etc*. (Fig. 1b). The outstanding property of these polymers is that they are converted to electrically conducting materials when "doped", either by oxidation or reduction in chemical terms (conductive state) (Fig. 1c).[6]

At the microscopic level, the doping process produces the appearance of intra-chain charged species which are stable due to the formation of quinoidal segments generated at the expense of the previously aromatic moieties. Polarons and bipolarons in heterocyclic-based conducting polymers reside on sizeable quinoidal structures which stabilize the charge and

Department of Physical Chemistry, University of Málaga, Málaga, Spain. E-mail: casado@uma.es, teodomiro@uma.es; Fax: +34 952132000; Tel: +34 952132018

Juan Casado

Juan Casado is Associate Professor of Physical Chemistry at the University of Málaga. He received his BSc and PhD in Chemistry at the same University in the field of Raman spectroscopy of oligothiophenes. Further research followed at University of Minnesota in Minneapolis in organic electrochemistry and spectroelectrochemistry. For two years he conducted spectroscopic studies at the Steacie Institute for Molecular Sciences at the NRC in Ottawa. His present research is focused on the analysis of the electronic structure of conjugated molecules with incidence in the mix valence behavior, diradicaloid properties, excited states interplay, non-linear optics, etc. Recent studies involve Raman and infrared vibrational dichroism. He is the author of around 150 original publications.

Rocío Ponce Ortiz

Rocío Ponce Ortiz was born in Marbella. She studied at the University of Málaga where she obtained her degree in Chemical Engineering in 2003 and PhD in Chemistry in 2008 in the Group of Spectroscopy of Molecular Materials headed by Prof. López Navarrete. She worked (2008–2011) as a post-doctoral fellow with Prof. Tobin Marks at Northwestern University (USA), under an IOF Marie Curie contract. After that, she joined the University of Malaga. Her current research is focused on the analysis of the electronic structure of conjugated molecules and their applications in thin-film transistors. She is the author of more than 40 original publications.

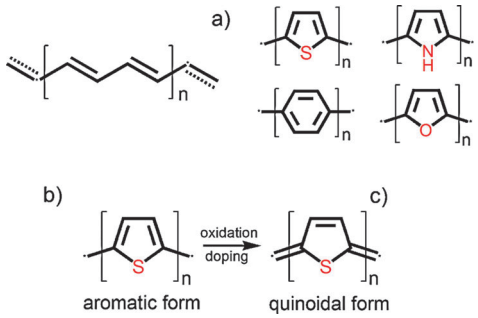

Fig. 1 (a) Conjugated structure in polyacetylene; (b) prototypical conducting polymers ($n = \infty$); and (c) aromatic-to-quinoidal conversion by oxidative doping.

infer them mobility due to the relatively easy aromatic ↔ quinoidal conversions.[7] The precise study of the electronic and molecular features of these quinoidal structures has been of interest since the discovery of conducting polymers.

The *Oligomer Approach* has provided an ideal framework to infer polymer properties by extrapolating those of the well-defined oligomers as a function of the oligomer length (see Fig. 2 for oligomeric charge defects models).[8–10] As such, the preparation of oligomers with well defined quinoidal structures has been a synthetic challenge pursuing their use as insightful models of the structure of polymeric polarons and bipolarons. In this review we will revise the main work done in the investigation of quinoidal oligomers as models of doped conducting polymers (Fig. 2). The family of polythiophenes is one of the most versatile and studied classes of conducting polymers, hence we will focus in polythiophene and therefore on quinoidal oligothiophenes as their oligomeric models.[11–14] The historical perspective of these quinoidal thiophenes will show that, nowadays, they are much more than mere doped polythiophene models and they constitute a highly useful example of investigation in organic electronics.

Juan T. López Navarrete

Juan T. López Navarrete is a Full Professor of Physical Chemistry and Head of the Central Research Services at the Universidad de Málaga. He received his BSc in Chemistry from the Universidad de Extremadura and the PhD in Chemistry from the Universidad de Málaga. He then worked as a postdoctoral fellow with Prof. G. Zerbi on Lattice Dynamics of Organic Conducting Polymers at the Politecnico di Milano. His research interests span a range of targets with emphasis on the application of vibrational and electronic spectroscopies, chiro-optical spectroscopies, electrochemistry and quantum chemical computations to the study of π-conjugated materials, carbon nanostructures and electroactive molecules. He is the author or co-author of over 230 original publications.

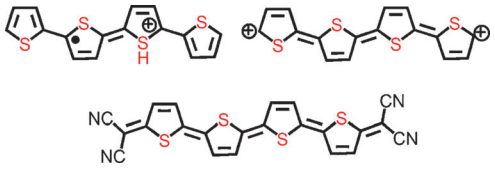

Fig. 2 Radical cation and dication of a quaterthiophene as oligomeric models of polaronic and bipolaronic residues, respectively, together with a tetracyano quinoidal quaterthiophene.

Years before the accidental discovery of polyacetylene (the first conducting polymer), the search of conductive materials based on organic molecules was intensively devoted to the so-called charge transfer salts.[15–19] These are based on electron donor and electron acceptor systems with interchange charge forming columns of aggregates, charged either positively or negatively, wherein charge transport can take place. The prototypical charge transfer salt is formed by the tetrathiafulvalene (TTF) electron donor and the tetracyanoquinodimethane (TCNQ) electron acceptor (Fig. 3).[19,20] The search for new TCNQ derivatives with improved properties in charge transfer salts led to the design of tetracyanoquinodimethane molecules substituting the central quinoid benzene ring by thiophene. This was the reason for the preparation of the first example of quinoidal oligothiophene based in the thiophene monomer or tetracyanoquinodimethane thiophene, **TCN1QT**.[21,22]

There are other quinoidal oligothiophenes not based on the tetracyano functionality, for example thiophene derivatives of the Thiele's hydrocarbon[23] or constituted by semiquinones at both free termini of the oligothiophene,[24–28] to cite just a few. In this review we will exclusively focus on the tetracyanoquinodimethane oligothiophene derivatives, and we will refer to them as quinoidal or TCNQ oligothiophenes. The most prominent reason for the choice of TCNQ oligothiophenes is that they represent one of the most versatile quinoidal thiophenic forms, as they have been used in different areas of chemistry and material science. Fruitful investigations of TCNQ oligothiophenes can be found in fields of research as diverse as organic electronics, diradical chemistry and magnetism, conducting polymers, non-linear optical materials and multiphotonic materials, *etc*.

The study of conducting polymers, and afterwards of conjugated oligomers, has been scrutinized in several ways by Raman spectroscopy.[30,31] Probably the main difference between inorganic and organic semiconductors resides in the role of the electron–phonon coupling in the organic materials which intimately correlates electron, or excitation dynamics,

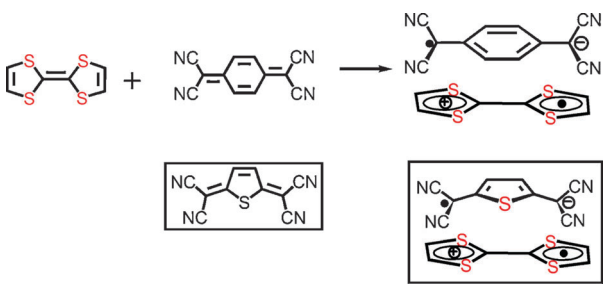

Fig. 3 Formation reaction of the charge-transfer salt of **TTF** and **TCNQ**. In the boxes, the analogue with thiophene, **TCN1QT**.

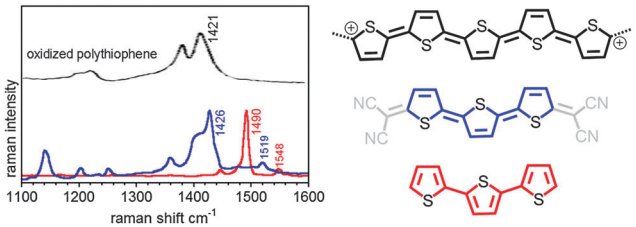

Fig. 4 Raman spectra of aromatic (red) and tetracyano quinoidal (blue) terthiophene with chemical structures in red and blue, respectively. The FT-Raman spectrum in black corresponds to heavily oxidized polythiophene from Lefrant *et al.*[29] Reprinted with permission from ref. 29. Copyright 1996, American Chemical Society.

with structural skeletal changes that happen in the molecule along particular vibrational modes. These vibrations are particularly enhanced in the vibrational Raman spectrum (see the strongest Raman bands in Fig. 4). In consequence, the search of a more complete understanding of the alteration of the molecular structure during optical excitations and with the doping load in conjugated molecules is the reason for the widespread use of Raman spectroscopy. Anticipated by the Amplitude Mode theory[32,33] in polyacetylene, the Effective Conjugation Coordinate model (ECC) by Zerbi *et al.*[30,34] had the particular approval of chemists for being able to translate into molecular properties (vibrational normal modes and molecular force constants) the physics of the electron–phonon mechanism. The ECC model has been broadly used to study the electronic and structural properties of conjugated molecules, being especially informative within the application of the *Oligomer Approach*.[35,36] The ECC model establishes the existence of a collective C=C/C–C mode (the C=C and C–C bonds simultaneously enlarge and shrink, respectively). The ECC mode conducts the electron–phonon mechanism and is featured by two main spectral signatures in the Raman spectrum: (i) the ECC mode is the strongest band of the spectrum, and (ii) the frequency of the ECC mode downshifts with the increase of conjugation that happens, among other circumstances, with the enlargement of the chain size in aromatic oligomers and with quinoidization of the backbone: see Fig. 4 for the downshift displacement of the strongest ECC mode with the quinoidization of the thiophene backbone.[37,38]

Our Raman studies of TCNQ oligothiophenes are based on the statements of the ECC theory and on the behaviour of the ECC mode.

The outline of the present *Tutorial Review* is divided in the following sections. Initially we pursue a first historical perspective of the many families of TCNQ oligothiophenes in the last 20–30 years of the 20th century. The beginning of the 21st century showed the emergence of these thienyl oligomers as semiconducting elements in organic electronics, and the third section will be devoted to this issue. The fourth section will deal with alternative ways to attain quinoidal thiophenes based on modifications of the tetracyanoquinodimethane solution. The use of TCNQ thiophenes is not restricted to the case of field-effect transistor devices, but a number of new optical and magnetic properties promise the exploitation of these samples as multifunctional substrates. The next three sections are devoted to factors relating to the appearance of diradical properties. The last two parts of the review are focused on the consideration of the knowledge gained with the TCNQ thiophenes to address the vibrational features of polaron pairs as alternatives to bipolarons in oxidized polythiophene, with special emphasis in the disruption of quinoidal stability. The review will close with the amazing future perspectives that we envisage for quinoidal oligothiophenes.

A significant part of the findings related with TCNQ thiophenes has been guided and supported by vibrational spectroscopic analysis, in particular, Raman spectroscopic data.[39] This forms the basis of this article by reviewing the main properties and applications of the TCNQ thienyl family of compounds in connection with the spectroscopic Raman features that have paralleled their research. The comprehensive knowledge of their Raman properties has allowed the understanding of the origin of their unconventional electronic properties, intrinsically associated with the concatenation of thienyl quinoidal rings and their partial stability.

Quinoidal oligothiophenes up to year 2000

One of the first examples of quinoidal oligothiophenes appeared in the late 1980s as alternatives to the tetracyanoquinodimethane

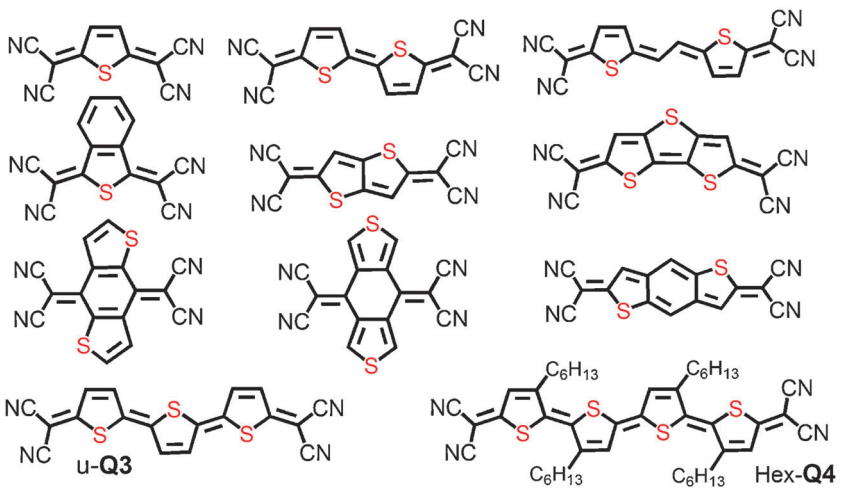

Fig. 5 Some examples of the first tetracyano quinoidal oligothiophenes synthesized as TCNQ alternatives.

(TCNQ) acceptor in conductive organic charge-transfer salts.[16,40] Fig. 5 shows a selection of first TCNQ oligothiophenes described in the literature.

At that time, interest was focussed in the search of new molecules with attenuated on-site Coulombic repulsion in order to enhance the reductive properties of TCNQ. Due to extended conjugation in oligothiophenes (lower aromatic character of thiophene compared to benzene), these were quickly considered as attractive TCNQ alternatives. In addition to the modulation of conjugation, the introduction of sulfur atoms with oligothiophenes acted advantageously on the formation of stacked molecular complexes since they promote beneficial intermolecular connections.

The following conclusions, extracted from the main studies about TCNQ oligothiophenes, will be useful for our ongoing discussion:[16,17,41,42] (i) quinoidal oligothiophenes have lower electron affinities compared to TCNQ, however the greater chemical versatility of thiophene represents a synthetic advantage due to the possibility of preparing long (up to with six thiophenes) oligomers and oligomers with a diversity of functionalizations. (ii) Complexes of TCNQ thiophenes with various electron donors often exhibit high electrical conductivities (eventually up to the metallic regime), partially addressed by the presence of sulfur atoms in the acceptor moieties which induce significant intermolecular interactions, forming sheet-like networks for charge transport. (iii) A structural aspect of importance concerns the facility of TCNQ thiophenes to undergo *cis–trans* isomerisation.[42] Aromatic oligothiophenes are robust molecules against isomerisation, principally due to the lower thermodynamic stability of the *cis* isomers and to the large energy cost of the *cis*→*trans* transition state.[43,44] However, the pro-aromaticity of TCNQ thiophenes stabilizes the transition state which, in conjunction with steric effects, can drive the formation of *cis* and *trans* mixtures (see Fig. 6). Experimental ^{1}H NMR and electronic absorption experiments in a TCNQ quinoidal bithiophene, substituted with two hexyl groups in Fig. 6, proved the evolution from an *all-trans* conformation to a mixture with *cis* conformers (Fig. 6). This work by Higuchi *et al.* represented the first clear indication of the role of diradical states in TCNQ oligothiophenes, an aspect of crucial relevance to understand the electronic properties of long quinoidal thiophenes, such as will be described in the next sections.[42] (iv) TCNQ oligothiophenes also display interesting optical properties. They are characterized by low-energy lying optical excitations, very intense electronic absorptions and large third-order hyperpolarizabilities.[41] The occurrence of these optical properties results from the activity of a charge transfer excitation mechanism associated with their acceptor–donor–acceptor chemical pattern. (v) The extension of the charge transfer property in the ground electronic state, or charge polarization from the central thiophenic donor towards the electron deficient dicyano groups, has been probed by IR and Raman spectroscopies based on the close relationship between the frequency position of the C≡N stretching modes and the charge density on the cyano groups.[39,45–47] This was the first use of vibrational spectroscopy in the characterization of TCNQ oligothiophenes. The second aspect in which vibrational Raman spectroscopy was used in the studies of TCNQ thiophenes was in the consideration of them as ideal oligomeric models of bipolarons.[48–50] Bipolarons can be described as quinoidal structural segments associated with the stabilization of the double positive (negative) charges in the oxidized (reduced) polymer. In this sense the well-defined quinoidal structure of TCNQ oligothiophenes (free of chemical and electronic defects) represented perfect oligomeric models of bipolarons of polythiophene. Fig. 4 shows the Raman spectrum of **u-Q3** (unsubstituted quinoidal terthiophene), which shows the main Raman peak at 1426 cm^{-1} is closely related with the most intense Raman band of heavily oxidized polythiophene around 1421 cm^{-1}, revealing the similar quinoidal structure of **u-Q3** and of bipolarons in doped polythiophene.[29,51]

Quinoidal oligothiophenes in organic electronics

Organic electronics appeared in the early 1980s as a cheap and versatile alternative to inorganic-based devices. The difference is that the semiconductor layer in the field-effect transistors (FET) is replaced by an organic one, which can be a polymer

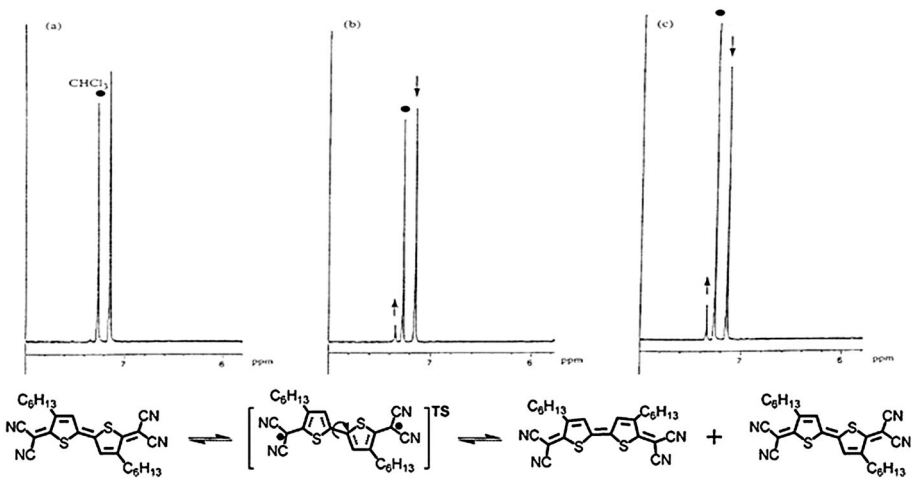

Fig. 6 Time evolution of the ^{1}H NMR spectra of the hexyl substituted TCNQ bithiophene and explanation in terms of *cis* ↔ *trans* isomerisation. Reprinted with permission from ref. 42. Copyright 1998, The Chemical Society of Japan.

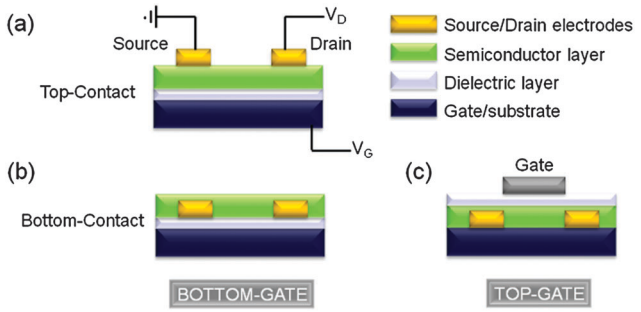

Fig. 7 Typical OFET architecture structures: (a) bottom-gate top-contact, (b) bottom-gate bottom-contact, and (c) top-gate bottom contact configurations.

or a small molecule. FETs are the fundamental parts of all electronic devices, and are characterized by the presence of an electric field that controls and modulates the conductivity of the active channel. The key FET performance parameters include the charge carrier mobility, μ, the threshold voltage, V_T, and the on/off current ratio, I_{ON}/I_{OFF}. In parallel with the inorganic parents, organic devices are also divided in two classes according to the sign of the charge carriers, either electrons or holes, which give rise respectively to n- or p-type charge transport. Most of the organic devices are p-type while n-type are in deficit due to the electron rich nature of poly-conjugated molecules.

Fig. 7 shows the different device configurations of a FET, in which three electrodes are present, source, drain and gate.[52] In this three-electrode configuration the gate electrode is the responsible of the creation of the electric field with respect to the source, or gate voltage, V_G. When $V_G = 0$, the device is "off". However, on increasing both V_G and V_D (voltage between the source and the drain electrodes, or drain voltage), a linear current regime is observed at low drain voltages ($V_D < V_G$) (eqn (1), linear regime) followed by a saturation regime at higher V_D values (eqn (2), saturation regime).

$$(I_{SD})_{lin} = (W/L)\mu C(V_G - V_T - V_D/2)V_D \quad (1)$$

$$(I_{SD})_{sat} = (W/2L)\mu C(V_G - V_T)^2 \quad (2)$$

In these equations, $(I_{SD})_{lin}$ stands for the drain current in the linear regime, $(I_{SD})_{sat}$ is the drain current in the saturation regime, μ is the field-effect mobility, W and L are the device channel width and length, respectively, and C is the capacitance per unit area of the insulator layer.

p-Type semiconductors with mobilities comparable to that of amorphous silicon in FETs have been already achieved. However, the development of n-type semiconductors with similar performances presents much more challenges.[53,54] Moreover, ambipolar semiconductors (able to transport both holes and electrons) are also required in order to simplify the design and fabrication of complementary metal-oxide semiconductor (CMOS) circuits.

The main strategy to obtain n-type organic semiconductors has been the design of electron deficient π-conjugated cores by functionalizing the electron-rich aromatic cores with electron-withdrawing groups, for example, the incorporation of cyano and perfluoroalkyl groups to oligothiophenes, naphthalenes or

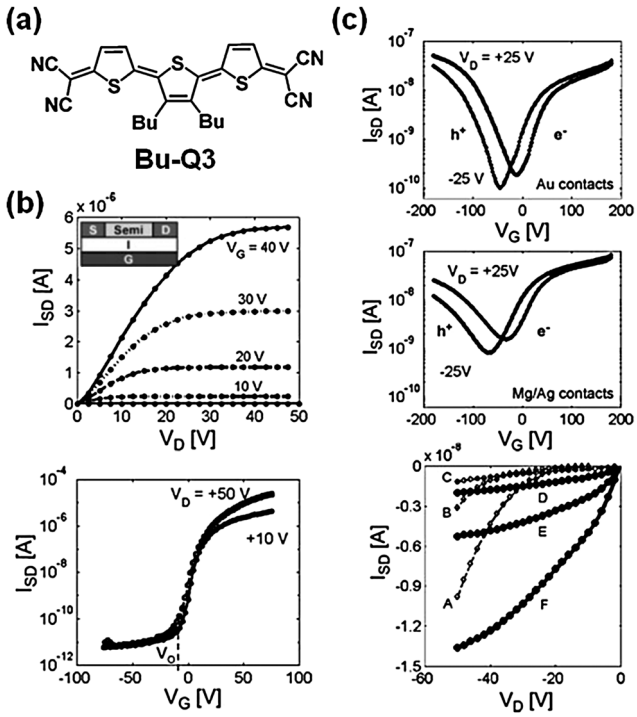

Fig. 8 (a) Chemical structure of quinoidal terthiophene **Bu-Q3**, (b) output and transfer characteristics for high n-channel mobility **Bu-Q3** thin film transistor (TFT), and (c) transfers and outputs characteristics for p- and n-channel (ambipolar) **Bu-Q3** TFT. Reprinted with permission from ref. 55. Copyright 2003, Wiley-VCH Verlag GmbH & Co. KGaA.

perylenes. In fact, the first n-type oligothiophenes were synthesized by Facchetti *et al.* by the introduction of perfluorohexyl or perfluoroarene groups to the conjugated skeletons.[35,56,57]

The idea of including strong electron-withdrawing dicyanomethylene groups (C=C(CN)$_2$ fragments) to thiophene backbones is more elaborate since it includes a twofold advantage, the electron deficient character together with the full planarization (quinoidization) of the thienyl core in TCNQ oligothiophenes. Pappenfus *et al.* first tested a TCNQ oligothiophene (terthiophene, **Bu-Q3** in Fig. 8) in an organic FET device which showed n-type behaviour with electron mobilities as high as 0.005 and 0.002 cm^2 V^{-1} s^{-1} for vapor- and solution-deposited films, respectively, in ambient conditions.[58] The dual electron-deficient and quinoidization effect induces a profound narrowing of the orbital HOMO–LUMO gap which simultaneously facilitates both oxidation and reduction processes (amphoteric redox behaviour), although this redox effect is only appreciable in TCNQ oligothiophenes with three or more thiophene units.[59] This redox property was exploited in optimized devices of **Bu-Q3**, obtaining a electron mobility up to 0.2 cm^2 V^{-1} s^{-1} together with hole mobility of $\sim 10^{-4}$ cm^2 V^{-1} s^{-1}, which represented one of the first unimolecular ambipolar organic semiconductors.[55]

The success on the discovery of the ambipolar charge transport behaviour of **Bu-Q3** was the consequence that followed the complete molecular level understanding of the strong chemical stability of the reduced (anions) charged species but also of the unexpected stability of the oxidized (cations) species of two similar TCNQ terthiophene and quaterthiophene molecules,

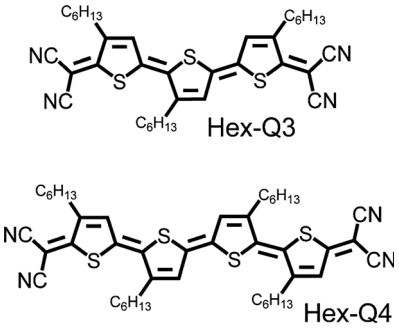

Fig. 9 Chemical structures of some quinoidal oligothiophenes.

Hex-Q3 and **Hex-Q4** in Fig. 9. We reported that the origin of this dual redox behaviour, and of the thermodynamic stability of these charged species, was rooted in the tendency of these quinoidal cores to become aromatic independently of the external redox stimulus, either oxidative or reductive.[59] Aromatization of the quinoidal core turns out to minimize chemical reactivity and favour long-term stability of the thus "aromatized" charged species. At the origin of the ambipolar behaviour, therefore, resides the pro-aromaticity of quinoidal backbones able to stabilize holes (radical cations) or electrons (radical anions) simply by changing the sign of V_G. As it will be seen in next sections, this strong pro-aromaticity property is the fundamental feature behind all the outstanding properties, such as represented in Fig. 10, which has allowed these compounds to become very promising organic electronic substrates.

The role of the butyl groups in the central thiophene of **Bu-Q3** not only results in an increased solubility but also promoted very good thin film molecular ordering. This was nicely demonstrated by the synthesis and OFET implementation of a TCNQ terthiophene bearing a bis(hexyloxymethyl)-cyclopentane unit fused to the central thiophene (**DHox-Q3** in Fig. 11). Within this approach the authors fabricated a solution-processed OFET with mobilities up to 0.16 $cm^2\ V^{-1}\ s^{-1}$ and $I_{on}/I_{off} \sim 10^3$ measured in ambient conditions.[60] For this oligomer, optimization of the annealing temperatures during device fabrication greatly increased the device performance, due to favoured crystallinity in the films.

One of the main drawbacks to the development of quinoidal derivatives with larger number of thiophene units, pursuing to stabilize further oxidations and reductions and improved ambipolarity, was the insolubility in common solvents.

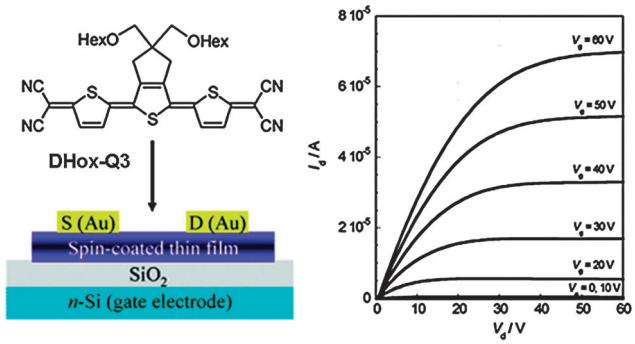

Fig. 11 Chemical structure of compound **DHox-Q3**, device architecture, and output characteristics of the **DHox-Q3**-based OFET. Reprinted with permission from ref. 60. Copyright 2007, American Chemical Society.

To overcome this, Takahashi *et al.* used a new lateral solubilising building block, bis(butoxymethyl)cyclopentane ring, fused to every thiophene unit. With this strategy Otsubo *et al.* were able to synthesize an aromatic oligothiophene with up to 96 units.[61] The preparation of larger quinoidal oligothiophenes with this strategy was successful, and oligomers up to an hexamer (Fig. 12) were prepared.[62] However these long quinoidal units were not active in OFETs likely due to the steric bulkiness of the solubilizing units and poor crystallinity in the solid state.

In this monomer-to-hexamer series of TCNQ oligothiophenes, Raman spectroscopy has allowed the discovery of one of the most outstanding structural and electronic transformations promoted exclusively by the length of the oligomer and without parallel in any other family of oligomeric poly-conjugated compounds. The Raman finding was the evolution from a conventional closed-shell electronic state to the development of a diradical ground electronic state. This will be the focus of the next sections of this review. We close here with some of the most modern TCNQ oligothiophenes implemented in OFETs.

Despite the lower solubility of longer and alkyl-substituted quinoidal oligothiophenes, derivatives of quaterthiophenes, have been extensively studied by Ribierre *et al.* as semiconductor substrates.[63–68] Diverse substitution patterns have been prepared as exemplified in Fig. 13. As a summary they obtained: (i) OFET electron mobilities of $5 \times 10^{-4}\ cm^2\ V^{-1}\ s^{-1}$ in ***OMe*-Hex-Q4**;[65] (ii) for ***i*-Hex-Q4**, with alkyl chains in

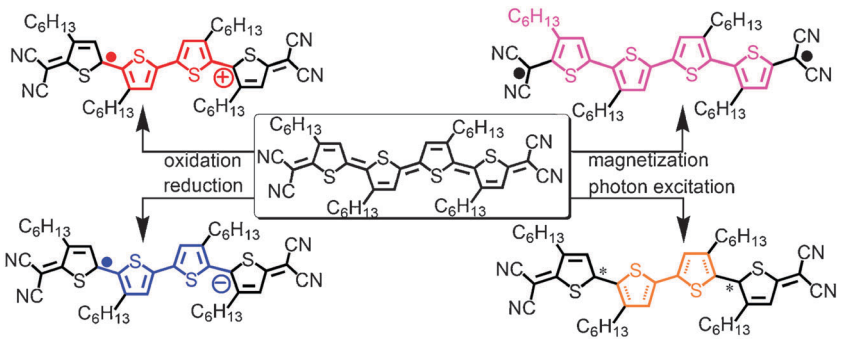

Fig. 10 Pro-aromaticity behaviour under external stimuli.

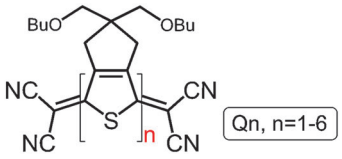

Fig. 12 Chemical structure of extended quinoidal oligothiophenes.

head-to-head configuration, ambipolarity with hole ($4 \pm 2 \times 10^{-3}$ cm^2 V^{-1} s^{-1}) and electron ($7 \pm 3 \times 10^{-2}$ cm^2 V^{-1} s^{-1}) field-effect mobilities was achieved in ambient conditions.[68] One very interesting discovery for ***i*-Hex-Q4** was the possibility to convert the type of charge carrier by simply thermal annealing. The authors showed that the temperature treatment conferred unaltered electron mobility but completely suppressed p-type current. Furthermore, since the fast development of this thermal effect (a few seconds at 180 °C), they were able to obtain the same charge carrier conversion by optically pumping the samples in their strongest absorption band by inducing local heating.[63,66] The potential of these results were demonstrated by the fabrication of CMOS-inverters on flexible polyethylenenaphthalene films, and NAND and NOR logic gates by both thermal annealing and laser writing techniques (Fig. 13).

In a subsequent communication,[64] the authors demonstrated that the majority carrier type in ***i*-Hex-Q4** thin films could be also controlled by the choice of the solvent used for the spin-coating process, reporting reversible conversion from n-type to ambipolar behavior by simple treatment with solvent vapours. These authors probed by Raman spectroscopy that the tuning of the electrical properties (by annealing, laser irradiation or solvent vapour exposition) should be associated to modification of the films properties, ruling out that these electrical changes were associated to modifications in the molecular quinoidal structure.

In a more recent contribution, the same authors went a step further and substituted the two external thiophene rings by selenophenes,[69] aiming at enhancing the intermolecular overlap by inclusion of more polarisable and larger selenium atoms.[70,71] In fact, this strategy had been already used in TCNQ-type quinoidal biselenophenes,[72] which show a slight enhancement of the electron mobility compared to the bithiophene homologous. For the TCNQ heteroquinoid derivative **DHox-Q3(Se)** in Fig. 14, however, the electron mobility was lower than that of **DHox-Q3**-based devices by one order of magnitude (1.6×10^{-2} cm^2 V^{-1} s^{-1} *vs.* 0.16 cm^2 V^{-1} s^{-1}), although hole mobility was increased to 7.0×10^{-3} cm^2 V^{-1} s^{-1}. In any case, owing to the fairly well balanced ambipolar transport in **DHox-Q3(Se)**-based OFETs, the authors examined CMOS-like inverters using two identical transistors on the same Si/SiO_2 substrate, obtaining a relevant gain of *ca.* 16 (Fig. 14).

The solid-state properties of the TCNQ quinoidal oligothiophenes deserve a special mention as it is well known that they critically influence the final electrical performance of electrical devices. Precise, straightforward and applicable rules able to relate the crystalline structure and the electrical or semiconducting performance are however far from established. Nonetheless, some particular solid-state organizations, in particular assemblies of co-facial π-stacking columns of molecules, definitively favour enhanced charge mobility.

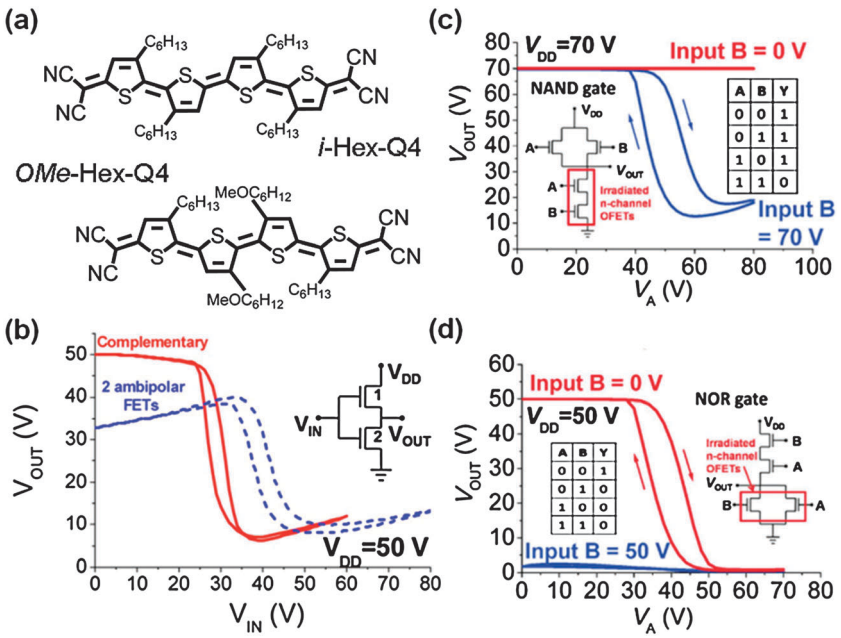

Fig. 13 (a) Chemical structures for ***OMe*-Hex-Q4** and ***i*-Hex-Q4** semiconductors. (b) Switching characteristics of flexible ***i*-Hex-Q4** inverters measured in ambient conditions. The dashed curve corresponds for a inverter composed of two pristine OFETs, whereas the solid curve was obtained with the combination of one pristine (transistor 1) and one thermally annealed n-type OFET (transistor 2). (c) Transfer characteristics of NAND logic gate and (d) NOR logic gate. The circuits for NAND and NOR logic gates were composed of two ambipolar p-dominant FETs and two laser irradiated n-type FETs. Insets show the circuit schematics and the truth tables. Reprinted with permission from refs. 63 and 68. Copyright 2010, American Institute of Physics, and Copyright 2010, Wiley-VCH Verlag GmbH & Co. KGaA.

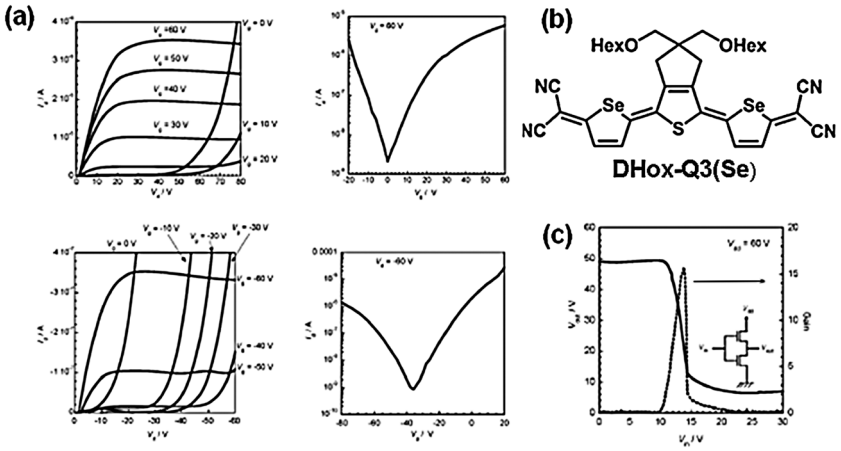

Fig. 14 (a) Ambipolar FET characteristics (left: output plot, right: transfer plot) of a **DHox-Q3(Se)**-based OFET annealed at 150 °C. (b) Chemical structure of **DHox-Q3(Se)**. (c) Transfer characteristics of its CMOS-like inverter. Reprinted from ref. 69. Reproduced by permission of the Royal Society of Chemistry.

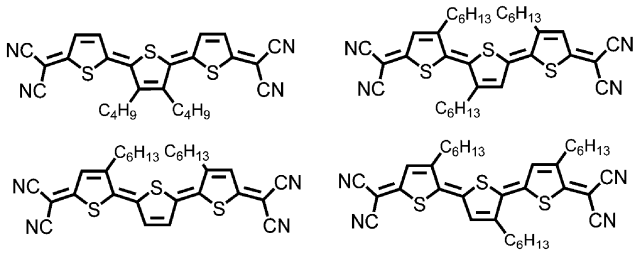

Fig. 15 TCNQ terthiophenes studied by Janzen *et al.*[73]

Janzen *et al.*[73] studied the crystalline structures of the four quinoidals in Fig. 15 and obtained repetitive structural motifs exploitable to design enhanced materials. Their X-ray structures display short intermolecular π-stacking distances around 3.4 Å. Also they show either parallel single π-stacking distances with parallel cofacial π-stacking, or alternating π-stacking distances and antiparallel π-stacking. These π-stack columns can be organized in layers or in herringbone motifs. In this study the authors correlate the solid-state ordering with relevant semiconducting parameters such as the charge-transfer integral or valence and conduction bandwidths obtained by accurate molecular orbital calculations. These crystalline orbital bandwidths are rather large both for the valence and for the conduction bands, supporting the ambipolar charge transport actuation.

Raman spectroscopy has also been utilized to explore the solid-state properties of these quinoidals. In particular for **Bu-Q3**, in going from the crystalline solid to dichloromethane solution, its main Raman bands largely up-shift by 8–10 cm^{-1}, an effect ascribed to the removal of the strong solid-state interactions and, in particular, to the disappearance of the donor–acceptor interaction between neighbouring molecules in the π-stack.[49] This donor–acceptor coupling in fact makes the π-stacking disposition in the quinoidals to be much closer than that of the charge transfer complexes (donor–acceptor salts) or even of π-dimers of oxidized aromatic terthiophenes likely resulting in the principal driving force of the crystallization of TCNQ oligothiophenes.

Quinoidal oligothiophenes: chemical modifications

As shown in the previous sections, the major strategy to achieve a quinoidal structure in oligothiophenes has been tetracyano-substitution. Other alternative motifs to attain quinoidization of oligothiophenes have been used pursuing the modulation of the electro-optical properties[24,27,28] or an enhanced processability.[74,75] There are two main examples that modify the tetracyano substitution, either partially or totally, to prepare quinoidal thiophenes, such as shown in Fig. 16.

Full replacement of cyano groups by quinones has been used by Zerbi and others[25–28] to prepare quinoidal bithiophenes (four quinoidal rings in total considering the two benzoquinone groups) with the focus in the exploitation of their non-linear optical properties. Due to their symmetric acceptor–donor–acceptor substitution and to the charge transfer character of their optical excitations, quinoidal dyes are promising candidates with large molecular polarizability and hyperpolarizability (β, γ) for materials with a large macroscopic non-linear response ($\chi^{(2)}$, $\chi^{(3)}$). Their symmetric character ($\mu \approx 0$) in addition represents an interesting avenue for macroscopic control of the NLO response.[28] This hetero-quaterphenoquinone molecule was used to fabricate a planar organic near infrared light detector.[24] Interestingly, these authors considered

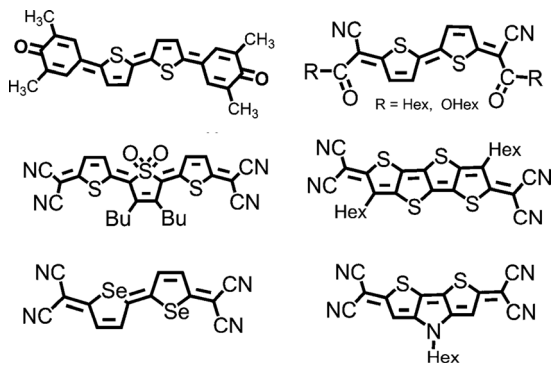

Fig. 16 Representative examples of quinoidal thiophenes with alternative TCNQ motifs and used in organic electronics.

the vibrational IR and Raman spectra of these quinoidals to estimate the magnitude of β and γ under the assumption of substantial vibrational contribution to the microscopic/molecular NLO properties.

Partial substitution of the dicyano group was attained by replacement of one of the two with a carbonyl group, either as ((alkyloxy)carbonyl) or as acyl groups (Fig. 16).[74,75] The incorporation of alkyl chains at the electron-withdrawing function led to increased processibility and control of the solid-state organization. This, however, has been at the expense of the electron acceptor strength of the quinoidal dye due to the substitution of C≡N by a weaker C=O acceptor. Nonetheless, the inclusion of the carbonyl function still keeps the LUMO energy level sufficiently low, around 4.0–4.2 eV below the vacuum level, thus meeting the criteria for air-stable n-type carrier transporting substrates in OFETs. In addition, for oligothiophenes with three or more thiophene rings, amphoteric behavior was also maintained as in the TCNQ analogues. For all these molecules electron mobilities were registered in the order of 10^{-2} cm^2 V^{-1} s^{-1},[74,75] and in the case of the quinoidal tetramers ambipolar FET characteristics were described with balanced hole and electron mobilities of $\sim 10^{-4}$ cm^2 V^{-1} s^{-1}.[74]

Other strategies of modifying TCNQ oligothiophenes were conceived by altering the thiophene moiety, which has been exploited in three main routes. The first deals with the combination/substitution of thiophenes by other five-membered rings, for instance, the alternation of thiophene and selenophene by Takimiya *et al.*[70,71,76] and thiophene and pyrrole by Pappenfus *et al.*[77] Casado *et al.*[78] conceived a second way of chemically modifying the thiophene function through the stabilization of a tetravalent state of the thienyl sulfur in its dioxide derivative, thus producing a stronger electron acceptor moiety. The idea behind the preparation of dioxide quinoidal dyes was the study of their emissive properties with the objective of combining ambipolar charge transporting materials with emissive properties in one sole substrate for organic light emitting transistors.[79,80] The *S*,*S*-dioxide insertion produces some interesting effects: (i) it deactivates the electron donor ability of the central sulfur, leading to competing intramolecular charge transfer as nicely characterized by Raman spectroscopy; (ii) it was also concluded that, concerning the emissive properties, the "flexible" character of the first excited state together with the intrinsically low S_0–S_1 gap were detrimental factors for the achievement of moderate fluorescent properties.[78]

Very recently another interesting chemical modification of the TCNQ thienyl core is the fusion of the rings such as in the thienoacene aromatic derivatives. Thienoacenes are completely fused and planar aromatic oligothiophenes. One of the beneficial effects of thienoacenes is the increase of ratio between the conjugated pz sulfur *vs.* carbon electrons in the donor core. A TCNQ thienoacene with four fused rings has been prepared and implemented in solution-processed OFET devices with mobilities up to 0.9 cm^2 V^{-1} s^{-1} and good ambient stability.[81]

Quinoidal oligothiophenes as multifunctional material candidates

Functional and multifunctional materials allude to those substrates able to simultaneously perform more than one operation or able to provide distinctive responses to different stimuli. We have already described the electrical versatility of TCNQ oligothiophenes as semiconductors. Now, additionally, we will describe two examples of TCNQ oligothiophenes with magnetic and optical properties as well.

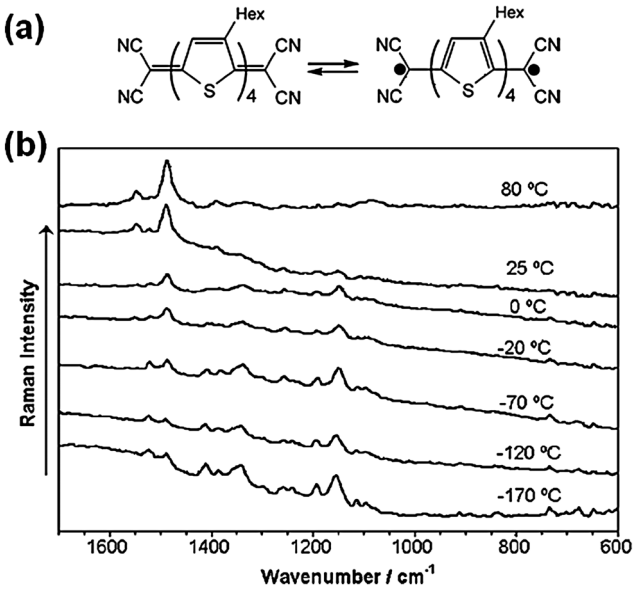

Fig. 17 (a) Equilibrium between the closed-shell quinoid structure and the diradical aromatic structure found at high temperatures for **Hex-Q4**. (b) 1064 nm FT-Raman spectra of solid **Hex-Q4** as a function of temperature. Reprinted with permission from ref. 82. Copyright 2006 Wiley-VCH Verlag GmbH & Co. KGaA.

We described in 2006 that the Raman spectrum of **Hex-Q4** irradiated with a 1064 nm Raman laser, reversibly changed on heating from room temperature to 80–100 °C (Fig. 17).[50,51] We ascribed this unusual behaviour to a reversible structural evolution from a quinoid-type pattern, that predominates at low temperature, to an aromatic-type pattern that prevails at higher temperatures. This effect was provoked by thermal $S_0 \rightarrow T_1$ intersystem crossing, leading to the population of the first open-shell pseudo-aromatic triplet state at the expense of the closed-shell quinoidal singlet state. This explanation highlighted two relevant insights: (i) the thermal accessibility of the magnetically active triplet excited state only 0.19 eV (4.38 kcal mol^{-1}) above the singlet ground-electronic state; and (ii) the strong stability of a diradical state (*i.e.*, triplet state) which becomes nearby the ground electronic state in **Hex-Q4**. This result was further supported by ESR experiments on the basis of the evolution of the ESR signal with temperature T which indicated two well differentiated regimes: (i) a Curie regime at low temperature typical of diamagnetic low spin singlet states (ST is almost constant, being S the ESR intensity and T the temperature), and (ii) a magnetic transition at higher temperatures (ST increases exponentially), typical of paramagnetic systems originated by the thermal population of a high spin triplet state.

Almost simultaneously to our work, in 2005, Takahashi *et al.* discovered the appearance of ESR activity at room temperature in CH_2Cl_2 solution of longer TCNQ oligothiophene derivatives, **Q5** and **Q6** (Fig. 12).[62] As will be discussed later,

both phenomena share the same diradicaloid origin. These findings are directly connected with the initial studies in the 1990s suggesting the existence of diradical transition states that could be responsible for the *cis–trans* isomerisation processes detected in short-chain TCNQ oligothiophenes (section B, Fig. 6). What we and Takahashi *et al*. discovered in longer quinoidals was that these diradical states rapidly become nearby the ground electronic state and are easily populated in normal conditions. The next section fully details the complete story of these diradicals. Just here, we wish to highlight the fact that, together with the enormous capacity to stabilize and transport charge, these molecules provide stable forms with a net spin momentum which can be potentially manipulated by external magnetic fields. This is very interesting for possible applications in spintronics, in addition to electronics.

In general, quinoidal molecules are very poor one-photon emitters with negligible fluorescence quantum yields (see dioxide case in section on quinoidal oligothiophenes: chemical modifications). Only bithiophenes weakly emit fluorescence. Very recently, however, Raymond *et al*.[83] have studied the photophysical properties of a TCNQ quinoidal bithiophene, **Q2** in Fig. 12, putting strong emphasis on the non-linear optical response and on the relevance of the photophysics of dark states such as observed in Fig. 18. Interestingly, they have found efficient two- and three-photon absorption features. In particular, the studied system is described an outstanding two-photon mediated three-photon emission which is visible by the naked eye. This represents one of the scarce examples of exploiting functional materials which feature intense and exclusive emissions induced by three-photon near-IR excitation. The authors have suggested that the occurrence of such an exceptional multiphoton property is due to the presence of an intense photon absorption (*i.e*., resonant absorption) from an intermediate level which is intensively two-photon absorptive thanks to its pronounced diradical character. Again the diradicalic property of TCNQ oligothiophenes makes a difference, in this case in the light absorption fingerprint.

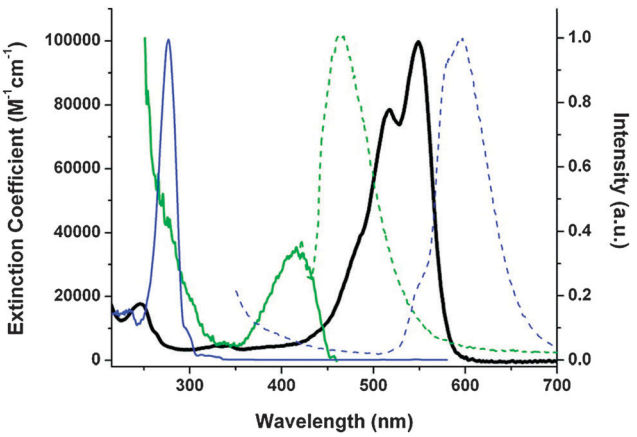

Fig. 18 Steady-state absorption (black) and emission/excitation spectra of **Q2**. The monomer-like excitation (solid green) and emission regime (dashed green) as well as the dimer-like excitation (solid blue) and emission (dashed blue) are given on the right axis. Reprinted with permission from ref. 83. Copyright 2011, American Chemical Society.

One of the latest developments in the research of solar cell devices is the exploitation of singlet fission in organic substrates. It turns out that the diradical species are perfect candidates for singlet fission processes due to the intrinsic connection between multiphoton absorption and singlet fission.[84] This is based on two intrinsic properties of diradicals: (i) they are usually strong absorbers in the NIR region; and (ii) given the proximity of the triplet states to the ground electronic state, it is verified that $E(S_1) > 2E(T_1)$, a requirement which is generally not easy to meet since in the most common chromophores the $E(S_1)$–$E(T_1)$ gap is considerably smaller than the $E(T_1)$–$E(S_0)$ gap. The shorter-membered TCNQ oligothiophenes are viable candidates that fully verify these opto-electronic and energy premises for singlet fission.

Quinoidal oligothiophenes: diradicaloid species

The largest, most complete and uniform series of TCNQ oligothiophenes (**Q*n*** in Fig. 12) is constituted by a set of five quinoidals where every thiophene ring is substituted by bis(butoxymethyl)-cyclopentane groups at their β positions, with the series encompassing up to a hexamer, **Q6**, that represents the longest quinoidal oligothiophene prepared so far.[85,86] Unfortunately, these materials are not electrically active in OFETs likely due to the bulky β-substitution which precludes solid-state π-stacking. The publication of these quinoidals in 2005 supposed three main findings: (i) the longest quinoidal ever synthesized, (ii) the translation of the strong electronic absorption bands characteristic of the quinoidal arrangement to the near-IR spectral region (this is relevant for photovoltaics), and (iii) the appearance of persistent ESR magnetic activity for the two longest members of the series, **Q5** and **Q6**. This magnetic result is an uncommon feature for molecules without any electron excess which, in principle, are electronically closed-shell neutrals. Raman spectroscopy enabled to comprehensively understand the electronic structural reasons behind this unconventional property. A description of the Raman behaviour of the perfectly chemically defined **Q*n*** oligothiophenes is described below.

Fig. 19 displays the Raman spectra of the **Q*n*** oligomers together with the spectra of the aromatic analogues, α,α′-dimethyl end-capped oligothiophenes,[87] up to the hexamer. The continuous frequency downshift of the ECC mode in aromatic oligomeric materials with the enlarging of the molecular size is well known (see band with arrows in Fig. 19), owing to the increase of π-electron delocalization, or conjugation, between the successive thiophene units. This conjugative effect is well known to be reflected in a variety of properties such as the red-shift of the absorption and emission wavelength maxima in the optical spectra, the shift to lower potentials of the oxidation processes, the overall planarization of the thienyl backbone, *etc*.

However, the strongest ECC Raman mode in **Q*n*** compounds shows an initial downshift from **Q2** to **Q4**, merely reflecting the increase of molecular C=C/C–C conjugation, whereas, rather unexpectedly, from **Q4** to **Q6** the ECC mode frequency upshifts. Overall, the ECC in the **Q*n*** series shows a "turning point" behaviour with the inflexion point at the level of the tetramer. In terms of molecular structures, we can assume

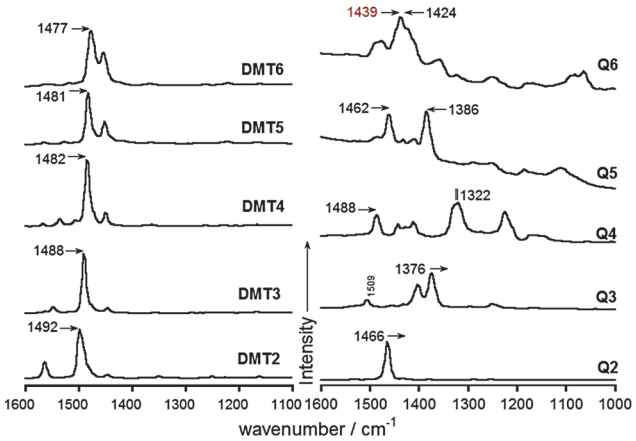

Fig. 19 1064 nm FT-Raman spectra of dimethyl aromatic oligothiophenes (**DMT*n***) and **Q*n*** quinoidal oligomers. Reprinted with permission from ref. 85. Copyright 2007, Wiley-VCH Verlag GmbH & Co. KGaA.

that in the aromatic oligothiophenes the chain length increase of π-conjugation might delineate a gaining of quinoidization of the ground electronic state. Conversely, one can think that in the quinoidal series a partial aromatization of the quinoidal structure for the longest members could take place what would explain the turning point ECC Raman behaviour: the question is why does this happen?

The answer can be inferred by supposing the Kekulé resonant forms and equilibrium in Fig. 20 which would explain: (i) the partial aromatization of the ground electronic state, which would be larger if the singlet open-shell diradical contribution is larger; and (ii) if the singlet open-shell diradical form is dominant in the description of the ground electronic state then, mandatorily, there exists an open-shell triplet diradical state very close in energy. This triplet excited state could be therefore thermally populated from the singlet diradical species simply by heating. This hypothesis would already account for: (i) the detection of magnetic ESR signals in solution for the longest **Q*n*** members by Takahashi *et al.* provided that the thermal energy at room temperature is

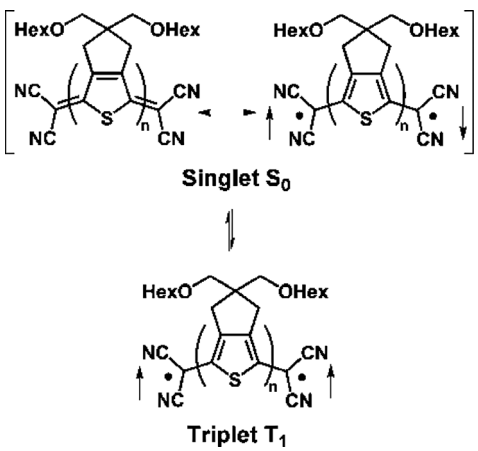

Fig. 20 Kekulé and diradical resonance structures for the singlet ground state of long quinoidal oligothiophenes in equilibrium with the triplet species.

enough to populate the magnetically active triplet state. and (ii) our variable-temperature FT-Raman spectra for **Hex-Q4** in Fig. 17 in terms of a diamagnetic (singlet)-to-paramagnetic (triplet) thermal magnetic transition. However, definitive evidence of the existence of these triplet states is elusive in terms of the half-field ESR signal; (iii) if aromatization by diradical formation happens only in the longest members, say **Q5** and **Q6**, therefore the turning point behaviour could be also elegantly explained. We now continue with Raman experimental evidence of the validity of our diradical hypothesis.

Fig. 21 displays the Raman spectra of **Q6** at different temperatures from −170 up to 130 °C where minor changes are observed on heating, indicating a very small S_0–T_1 energy gap which makes both states to have similar populations and precluding any significant thermal drain from one to the other. Conversely, the Raman spectra for **Q4** displays greater changes evolving from a Raman quinoidal profile at −170 °C (ECC mode below 1400 cm^{-1}) to a predominant aromatic profile at 130 °C (*i.e.*, ECC mode between 1450–1500 cm^{-1}) indicating: (i) a larger S_0–T_1 energy gap in **Q4** allowing singlet to triplet drain by heating. Furthermore this large S_0–T_1 gap makes the singlet ground electronic state very slightly diradicaloid, or mostly quinoidal (spectrum at −170 °C) while the triplet species is clearly pseudo-aromatic, such as noted by its +130 °C Raman spectrum.

Another proof of the singlet–triplet interplay comes from the resonant Raman spectra at room temperature obtained with the 514 nm laser. This laser excitation energy is right at the absorption energy of the triplet species present at room temperature for **Q6**. This spectrum, in Fig. 21, displays a pseudo-aromatic profile such as described for the triplet diradical form. Fig. 21 also compares the 1064 nm FT-Raman spectrum of **Q6** with the FT-Raman spectrum of the radical cation of the aromatic dimethylsexithiophene (*i.e.*, **DMT6**$^{+\bullet}$)[88] revealing a great similarity. It is well known that the **DMT6**$^{+\bullet}$ species is featured by a quinoidization of the central part of the molecule while the molecular extremes are pseudo-aromatic. This structural description is opposite to that of **Q6** in the sense that the pseudo-aromatization now is attained in the molecular center (*i.e.*, due to diradicaloid contribution) while its terminal rings remain quinoidal. Taking into account that the ECC mode accounts for the whole molecular structure, given its collective C=C/C−C stretching character, then the ECC frequencies in these two compounds are rather similar because the two molecular structures, on average, are also similar.

The use of theoretical model chemistry in these long quinoidal molecules proved to be challenging, in particular the prediction of the vibrational Raman spectra. In this regard, Fazzi *et al.*[89,90] provided a route to predict them, by combining at the DFT level the correct UB3LYP geometries (that calculated for the open-shell diradical) and performing the Raman activity calculations with a restricted wavefunction (that of the closed shell structure). In doing this, they predicted the turning point behaviour of the ECC mode frequency in the Raman spectra of our **Q*n*** oligomers. The arguments of the authors in this approach relies on the fact that the unrestricted wavefunction is spin contaminated, a fact irrelevant for the evaluation of

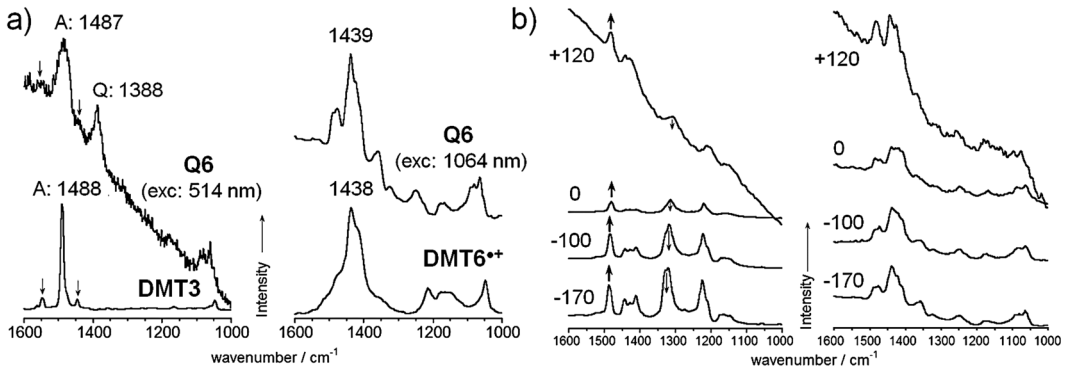

Fig. 21 (a) Raman spectra of **Q6** with excitation at 514 (top left), **DMT3** (excitation at 1064 nm, bottom left), **Q6** with excitation at 1064 nm (top right), and radical cation of **DMT6** (excitation at 1064, bottom right). A and Q denote typical aromatic and quinoidal bands, respectively. (b) Raman spectra as a function of temperature (in °C) for **Q4** (left) and **Q6** (right). Reprinted with permission from ref. 85. Copyright 2007, Wiley-VCH Verlag GmbH & Co. KGaA.

the structures, but critical for the estimation of the more elaborate molecular polarisabilities. The suppression of the spin contamination by using the restricted wavefunction seems to solve the problem. Nonetheless, this situation underlines the structural complexity of these TCNQ oligothiophenes and of the surprising effects that the presence of diradicaloid species brings to these challenging molecules, half-way between aromatic and quinoidals.

Quinoidal oligothiophenes: polaron-pair dications

Recently, we have used the relationship between the formation of diradicaloid species in TCNQ oligothiophenes and the Raman ECC frequency turning point behaviour to address one of the "perpetual" questions concerning the nature of the microscopic charge defects operating in conducting polymers, in doped polythiophene in particular.[91] As described in the Introduction, there are two main charge carriers: polarons (single charged units) and bipolarons (double charged units), depending of the doping load in the polymer. In the case of oligomers, oligothiophenes for polythiophene, radical cations and dications are the analogue charge defects of polarons and bipolarons, respectively.

The profound structural modification in bipolarons have led to an argument as to whether these double charged species would split into two interacting polarons in order to relax the structural strain in the polymer skeleton, or polaron pairs.[92] To provide new insights on the polaron pair formation, we have recently studied three aromatic oligothiophenes with six (**6T**), eight (**8T**) and twelve (**12T**) thiophenes and oxidized them to their dication forms (**D*n***) in Fig. 22) as models of bipolarons. As in the case of the TCNQ oligomers, we predict that for the longest members the quinoidization might be unstable and would undergo closed-shell aperture giving rise to singlet open-shell diradicals. It turns out that these diradicals are polaron pairs as represented in Fig. 22.

The Raman spectra of the neutral, radical cation and dication species of the three molecules are shown in Fig. 23

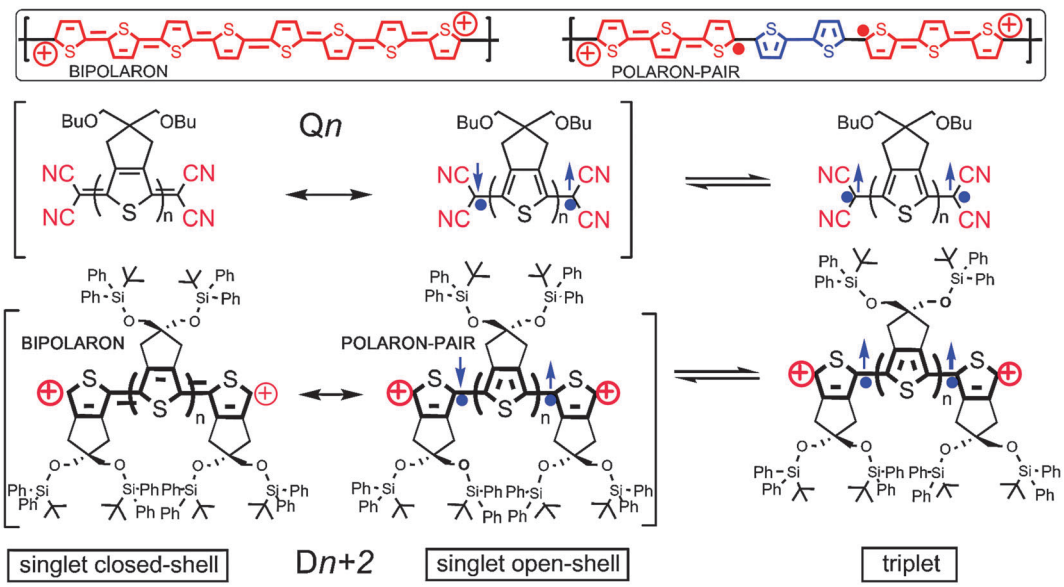

Fig. 22 (Top) Representation of the bipolaron and polaron-pair structures in polythiophene. (Bottom) Chemical structures of the **Q*n*** (n = 2–6) oligothiophenes and of the oligothiophene dications **D*n*+2** (4, 6, 10).

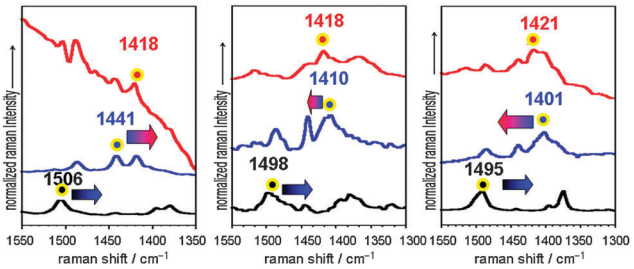

Fig. 23 Raman spectra of neutral (black), radical cation (blue) and dication (red) of **6T** (left), **8T** (middle) and **12T** (right). The arrows mark the ECC turning point behaviour. Reprinted with permission from ref. 91. Copyright 2011, American Chemical Society.

in which the frequency of the most intense ECC mode is marked. For the hexamer, there is a continuous downshift of the ECC mode with the oxidation degree in accordance with the appearance of a quinoidal path on one-electron oxidation (**6T** → **6T**$^{+\bullet}$) and a further extension of the quinoidization in the dication (**6T**$^{+\bullet}$ → **6T**$^{2+}$) to diminish charge repulsion. For **12T**, the behaviour is rather opposite: on **12T** → **12T**$^{+\bullet}$ the ECC mode frequency downshifts, whereas on passing to the dication this up-shifts significantly. This ECC turning point finding with oxidation is also advertised in **8T** with the oxidation level. Such as in the TCNQ oligothiophenes, we have ascribed this Raman behaviour to the formation of diradical species characterized by the aromatization of the molecular center which is responsible for the turning point ECC mode behaviour. It turns out that these diradical dications are polaron pairs and this Raman behaviour is the vibrational fingerprint of their formation. Further confirmation of the diradicaloid character of **12T**$^{2+}$ was provided by the detection of the triplet species in thermal equilibrium also by Raman spectroscopy.

The characterization of the diradical dicationic polaron pairs in long oligothiophenes is insightful about the forces that promote the formation of these diradicals in quinoidized oligothiophenes. Fig. 24 shows the evolution of the stabilization energy of the diradical form considered as the difference between its energy formation and that of the closed shell system. These energy data correspond to DFT calculations

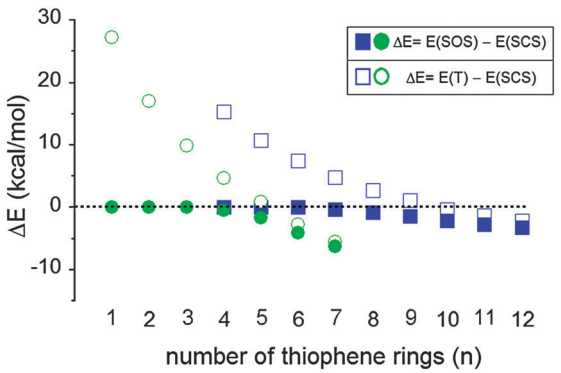

Fig. 24 DFT/(U)B3LYP/6-31G** relative ΔE energies (kcal mol^{-1}) between the triplet (T), singlet closed-shell (SCS) and singlet open shell (SOS) for the dicationic series (**D***n* + **2**, squares) and TCNQ oligothiophene series (**Q***n*, circles). Reprinted with permission from ref. 91. Copyright 2011, American Chemical Society.

by using the broken symmetry UB3LYP/6-31G** option for the open-shell diradical and the RB3LYP/6-31G** level for the closed-shell structures. $\Delta E = 0$ marks the end of the quinoidal stability, meaning that for shorter oligomers, quinoidization is the preferred format to stabilize TCNQ substitution or to accommodate two charges in a single molecule in the case of the diradical dications. For longer members, the molecules prefer to gain aromaticity paying the energy cost to break a double bond and to form a diradical. It turns out again that pro-aromaticity of quinoidal thiophenes promotes diradical formation; however, it occurs only when the molecular size surpasses a given chain length, or a chain length that contains a sufficient number of thiophenes, so that the energy sum by their individual aromatization surpasses the energy penalty to destroy a double bond giving rise to the diradical. The closed-shell to open-shell transition takes place at smaller chain lengths in TCNQ oligothiophenes than in the dications since the electron-withdrawal effect of the TCNQ groups contributes to weaken the strength of the double bond needed to be removed.

Quinoidal oligothiophenes: perspectives and challenges

The future of quinoidal molecules seems to be through the exploitation of their multiphotonic properties, still at a very initial stage. Possibly the elucidation of the capacity for two-photon, or multiphoton absorption, could be the driving force for their use in photovoltaics as they can be viewed as candidates for singlet fission process and multi-charge carrier formation. This, in combination with their inherent strong absorption in the NIR infrared region, can be attractive features for further investigation. It seems that their application as electro-active ambipolar transporters has achieved an optimal situation as for design of new chemical structures is concerned. However, there is still much room for material processing to obtain better performances. Their application in spintronics is a topic that, to our opinion, can be addressed soon.

We have tried to review the existing investigation on TCNQ oligothiophenes with emphasis on those used in organic electronics, in particular of n-type and ambipolar semiconducting materials. The revision of the electronic and structural properties of these promising compounds has been paralleled by the findings contributed by the use of Raman spectroscopy, mainly by our research group. The most fascinating property of these compounds is the diradical transformation with the chain length as a result of the balance of several forces (aromatization, electron-withdrawal effect, donor–acceptor coupling, *etc.*). The presence of stable diradicals is evidenced in the longest members, but for the shorter analogues the diradicals participate as low energy lying excited states which are responsible for surprising linear, non-linear and multiphotonic properties. Diradical states either in the proximity of the ground electronic state or in photon-accessible excited states are everywhere in the picture of quinoidal oligothiophenes. The ultimate reason of these features is the propensity of the quinoidal ring to share $4n + 2$ electrons in an aromatic manner.

Acknowledgements

This work was supported by the Ministerio de Educación y Ciencia (MEC) of Spain and by FEDER funds (project CTQ2009-10098 and to the Junta de Andalucía for the research project PO9-4708). R. P. O. thanks the European Community's Seventh Framework Programme (Grant Agreement 234808) for an IOF Marie-Curie contract.

References

1 A. G. MacDiarmid, *Angew. Chem., Int. Ed.*, 2001, **40**, 2581–2590.
2 A. J. Heeger, *Angew. Chem., Int. Ed.*, 2001, **40**, 2591–2611.
3 S. R. Forrest and M. E. Thompson, *Chem. Rev.*, 2007, **107**, 923–925.
4 M. Petty, *Molecular Electronics: From Principles to Practice*, John Wiley and Sons, 2008.
5 *Handbook of Conducting Polymers*, ed. T. A. Skotheim, R. L. Elsenbaumer and J. R. Reynolds, CRC Press, Third Edition, 2007.
6 H. Klauk, *Organic Electronics: Materials, Manufacturing and Applications*, Wiley-VCH, Weinheim, 2006.
7 J. L. Brédas, *J. Chem. Phys.*, 1985, **82**, 3808.
8 S. S. Zade, N. Zamoshchik and M. Bendikov, *Acc. Chem. Res.*, 2011, **44**, 14–24.
9 *Handbook of Thiophene-based Materials: Applications in Organic Electronics and Photonics*, ed. I. F. Perepichka and D. F. Perepichka, Wiley, Weinheim, 2009.
10 *Electronic Materials: The Oligomer Approach*, ed. K. Müllen and G. Wegner, Wiley-VCH, Weinheim, 1998.
11 J. Roncali, *Chem. Rev.*, 1997, **97**, 173–206.
12 A. Mishra, C.-Q. Ma and P. Bäuerle, *Chem. Rev.*, 2009, **109**, 1141–1276.
13 I. F. Perepichka, D. F. Perepichka, H. Meng and F. Wudl, *Adv. Mater.*, 2005, **17**, 2281–2305.
14 *Handbook of Oligo- and Polythiophenes*, ed. D. Fichou, Wiley, Weinheim, 1999.
15 H. Akamatu, H. Inokuchi and Y. Matsunaga, *Nature*, 1954, **173**, 168–169.
16 K. Yui, Y. Aso, T. Otsubo and F. Ogura, *Bull. Chem. Soc. Jpn.*, 1989, **62**, 1539–1546.
17 K. Yui, H. Ishida, Y. Aso, T. Otsubo, F. Ogura, A. Kawamoto and J. Tanaka, *Bull. Chem. Soc. Jpn.*, 1989, **62**, 1547–1555.
18 L. B. Coleman, M. J. Cohen, D. J. Sandman, F. G. Yamagishi, A. F. Garito and A. J. Heeger, *Solid State Commun.*, 1973, **12**, 1125–1132.
19 F. Wudl, D. Wobschall and E. J. Hufnagel, *J. Am. Chem. Soc.*, 1972, **94**, 670–672.
20 J. Ferraris, D. O. Cowan, V. Walatka and J. H. Perlstein, *J. Am. Chem. Soc.*, 1973, **95**, 948–949.
21 M. L. Kaplan, *J. Phys. Chem.*, 1980, **84**, 981.
22 *Handbook of Organic Conductive, Molecules and Polymers*, ed. H. S. Nalwa, Wiley, 1997.
23 T. Kawase, N. Ueno and M. Oda, *Tetrahedron Lett.*, 1992, **33**, 5405–5408.
24 T. Agostinelli, M. Caironi, D. Natali, M. Sampietro, G. Dassa, E. V. Canesi, C. Bertarelli, G. Zerbi, J. Cabanillas-Gonzalez, S. De Silvestri and G. Lanzani, *J. Appl. Phys.*, 2008, **104**, 114508.
25 K. Takahashi, T. Suzuki, K. Akiyama, Y. Ikegami and Y. Fukazawa, *J. Am. Chem. Soc.*, 1991, **113**, 4576–4583.
26 K. Takahashi, S. Fujita, K. Akiyama, M. Miki and K. Yanagi, *Angew. Chem., Int. Ed.*, 1998, **37**, 2484–2487.
27 F. D'Amore, M. Lanata, M. C. Gallazzi and G. Zerbi, *Chem. Phys. Lett.*, 2003, **377**, 243–248.
28 M. Lanata, C. Bertarelli, M. C. Gallazzi, A. Bianco, M. Del Zoppo and G. Zerbi, *Synth. Met.*, 2003, **138**, 357–362.
29 G. Louarn, M. Trznadel, J. P. Buisson, J. Laska, A. Pron, M. Lapkowski and S. Lefrant, *J. Phys. Chem.*, 1996, **100**, 12532.
30 C. Castiglioni, M. Tommasini and G. Zerbi, *Philos. Trans. R. Soc. London, Ser. A*, 2004, **362**, 2425–2459.
31 Y. Furukawa, A. Sakamoto, H. Ohta and M. Tasumi, *Synth. Met.*, 1992, **49**, 335–340.
32 B. Horovitz, *Solid State Commun.*, 1982, **41**, 729–734.
33 E. Ehrenfreund, Z. Vardeny, O. Brafman and B. Horovitz, *Phys. Rev. B*, 1987, **36**, 1535–1553.
34 C. Castiglioni, J. T. Lopez Navarrete, G. Zerbi and M. Gussoni, *Solid State Commun.*, 1988, **65**, 625–630.
35 J. Casado, V. Hernández, M. C. Ruiz Delgado, R. P. Ortiz, J. T. López Navarrete, A. Facchetti and T. J. Marks, *J. Am. Chem. Soc.*, 2005, **127**, 13364–13372.
36 J. Casado, S. Hotta, V. Hernández and J. T. López Navarrete, *J. Phys. Chem. A*, 1999, **103**, 816–822.
37 J. Casado, V. Hernández, S. Hotta and J. T. L. Navarrete, *Adv. Mater.*, 1998, **10**, 1458–1461.
38 J. Casado, M. Z. Zgierski, R. G. Hicks, D. J. T. Myles, P. M. Viruela, E. Ortí, M. C. Ruiz Delgado, V. Hernández and J. T. López Navarrete, *J. Phys. Chem. A*, 2005, **109**, 11275–11284.
39 V. Hernández, S. C. Losada, J. Casado, H. Higuchi and J. T. López Navarrete, *J. Phys. Chem. A*, 2000, **104**, 661–672.
40 P. W. Anderson, P. A. Lee and M. Saitoh, *Solid State Commun.*, 1973, **13**, 595–598.
41 H. Higuchi, T. Nakayama, H. Koyama, J. Ojima, T. Wada and H. Sasabe, *Bull. Chem. Soc. Jpn.*, 1995, **68**, 2363–2377.
42 H. Higuchi, S. Yoshida, Y. Uraki and J. Ojima, *Bull. Chem. Soc. Jpn.*, 1998, **71**, 2229–2237.
43 L. DeWitt, G. J. Blanchard, E. LeGoff, M. E. Benz, J. H. Liao and M. G. Kanatzidis, *J. Am. Chem. Soc.*, 1993, **115**, 12158–12164.
44 J. C. Horne, G. J. Blanchard and E. LeGoff, *J. Am. Chem. Soc.*, 1995, **117**, 9551–9558.
45 J. Casado, R. P. Ortiz, M. C. Ruiz Delgado, R. Azumi, R. T. Oakley, V. Hernández and J. T. López Navarrete, *J. Phys. Chem. B*, 2005, **109**, 10115–10125.
46 R. Ponce Ortiz, J. Casado, S. Rodríguez González, V. Hernández, J. T. López Navarrete, P. M. Viruela, E. Ortí, K. Takimiya and T. Otsubo, *Chem.–Eur. J.*, 2010, **16**, 470–484.
47 J. S. Chappell, A. N. Bloch, W. A. Bryden, M. Maxfield, T. O. Poehler and D. O. Cowan, *J. Am. Chem. Soc.*, 1981, **103**, 2442–2443.
48 A. Berlin, S. Grimoldi, G. Zotti, R. M. Osuna, M. C. Ruiz Delgado, R. P. Ortiz, J. Casado, V. Hernández and J. T. López Navarrete, *J. Phys. Chem. B*, 2005, **109**, 22308–22318.
49 J. Casado, T. M. Pappenfus, K. R. Mann, E. Ortí, P. M. Viruela, B. Milián, V. Hernández and J. T. López Navarrete, *ChemPhysChem*, 2004, **5**, 529–539.
50 T. M. Pappenfus, J. D. Raff, E. J. Hukkanen, J. R. Burney, J. Casado, S. M. Drew, L. L. Miller and K. R. Mann, *J. Org. Chem.*, 2002, **67**, 6015–6024.
51 V. Hernández, S. Hotta and J. T. López Navarrete, *J. Chem. Phys.*, 1998, **109**, 2543.
52 R. Ponce Ortiz, A. Facchetti and T. J. Marks, *Chem. Rev.*, 2010, **110**, 205–239.
53 J. E. Anthony, A. Facchetti, M. Heeney, S. R. Marder and X. W. Zhan, *Adv. Mater.*, 2010, **22**, 3876–3892.
54 X. W. Zhan, A. Facchetti, S. Barlow, T. J. Marks, M. A. Ratner, M. R. Wasielewski and S. R. Marder, *Adv. Mater.*, 2011, **23**, 268–284.
55 R. J. Chesterfield, C. R. Newman, T. M. Pappenfus, P. C. Ewbank, M. H. Haukaas, K. R. Mann, L. L. Miller and C. D. Frisbie, *Adv. Mater.*, 2003, **15**, 1278–1282.
56 A. Facchetti, Y. Deng, A. Wang, Y. Koide, H. Sirringhaus, T. J. Marks and R. H. Friend, *Angew. Chem., Int. Ed.*, 2000, **39**, 4547–4551.
57 A. Facchetti, M.-H. Yoon, C. L. Stern, H. E. Katz and T. J. Marks, *Angew. Chem., Int. Ed.*, 2003, **42**, 3900–3903.
58 T. M. Pappenfus, R. J. Chesterfield, C. D. Frisbie, K. R. Mann, J. Casado, J. D. Raff and L. L. Miller, *J. Am. Chem. Soc.*, 2002, **124**, 4184–4185.
59 J. Casado, L. L. Miller, K. R. Mann, T. M. Pappenfus, H. Higuchi, E. Orti, B. Milian, R. Pou-Amerigo, V. Hernandez and J. T. L. Navarrete, *J. Am. Chem. Soc.*, 2002, **124**, 12380–12388.
60 S. Handa, E. Miyazaki, K. Takimiya and Y. Kunugi, *J. Am. Chem. Soc.*, 2007, **129**, 11684–11685.
61 T. Izumi, S. Kobashi, K. Takimiya, Y. Aso and T. Otsubo, *J. Am. Chem. Soc.*, 2003, **125**, 5286–5287.
62 T. Takahashi, K.-i. Matsuoka, K. Takimiya, T. Otsubo and Y. Aso, *J. Am. Chem. Soc.*, 2005, **127**, 8928–8929.
63 J. C. Ribierre, T. Fujihara, S. Watanabe, M. Matsumoto, T. Muto, A. Nakao and T. Aoyama, *Adv. Mater.*, 2010, **22**, 1722–1726.

64 J. C. Ribierre, S. Watanabe, M. Matsumoto, T. Muto, A. Nakao and T. Aoyama, *Adv. Mater.*, 2010, **22**, 4044–4048.
65 J. C. Ribierre, T. Aoyama, S. Watanabe, J. Gu, T. Muto, M. Matsumoto, A. Nakao and T. Wada, *Jpn. J. Appl. Phys.*, 2010, 49.
66 J. C. Ribierre, T. Fujihara, T. Muto and T. Aoyama, *Org. Electron.*, 2010, **11**, 1469–1475.
67 J. C. Ribierre, T. Fujihara, T. Muto and T. Aoyama, *Appl. Phys. Lett.*, 2010, **96**.
68 J. C. Ribierre, S. Watanabe, M. Matsumoto, T. Muto and T. Aoyama, *Appl. Phys. Lett.*, 2010, **96**.
69 S. Handa, E. Miyazaki and K. Takimiya, *Chem. Commun.*, 2009, 3919–3921.
70 K. Takimiya, Y. Kunugi, Y. Konda, N. Niihara and T. Otsubo, *J. Am. Chem. Soc.*, 2004, **126**, 5084–5085.
71 T. Yamamoto and K. Takimiya, *J. Am. Chem. Soc.*, 2007, **129**, 2224–2225.
72 Y. Kunugi, K. Takimiya, Y. Toyoshima, K. Yamashita, Y. Aso and T. Otsubo, *J. Mater. Chem.*, 2004, **14**, 1367–1369.
73 D. E. Janzen, M. W. Burand, P. C. Ewbank, T. M. Pappenfus, H. Higuchi, D. A. da Silva Filho, V. G. Young, J.-L. Brédas and K. R. Mann, *J. Am. Chem. Soc.*, 2004, **126**, 15295–15308.
74 Y. Suzuki, E. Miyazaki and K. Takimiya, *J. Am. Chem. Soc.*, 2010, **132**, 10453–10466.
75 Y. Suzuki, M. Shimawaki, E. Miyazaki, I. Osaka and K. Takimiya, *Chem. Mater.*, 2011, **23**, 795–804.
76 T. Izawa, E. Miyazaki and K. Takimiya, *Chem. Mater.*, 2009, **21**, 903–912.
77 T. M. Pappenfus, B. J. Hermanson, T. J. Helland, G. G. W. Lee, S. M. Drew, K. R. Mann, K. A. McGee and S. C. Rasmussen, *Org. Lett.*, 2008, **10**, 1553–1556.
78 J. Casado, M. Z. Zgierski, P. C. Ewbank, M. W. Burand, D. E. Janzen, K. R. Mann, T. M. Pappenfus, A. Berlin, E. Perez-Inestrosa, R. P. Ortiz and J. T. L. Navarrete, *J. Am. Chem. Soc.*, 2006, **128**, 10134–10144.
79 M. Muccini, *Nat. Mater.*, 2006, **5**, 605–613.
80 R. Capelli, S. Toffanin, G. Generali, H. Usta, A. Facchetti and M. Muccini, *Nat. Mater.*, 2010, **9**, 496–503.
81 Q. Wu, R. Li, W. Hong, H. Li, X. Gao and D. Zhu, *Chem. Mater.*, 2011, **23**, 3138–3140.
82 R. P. Ortiz, J. Casado, V. Hernandez, J. T. L. Navarrete, E. Orti, P. M. Viruela, B. Milian, S. Hotta, G. Zotti, S. Zecchin and B. Vercelli, *Adv. Funct. Mater.*, 2006, **16**, 531–536.
83 J. E. Raymond, J. Casado, J. T. Lopez Navarrete, K. Takimiya and T. Goodson, *J. Phys. Chem. Lett.*, 2011, **2**, 2179–2183.
84 T. Minami and M. Nakano, *J. Phys. Chem. Lett.*, 2012, **3**, 145–150.
85 R. Ponce Ortiz, J. Casado, V. Hernandez, J. T. Lopez Navarrete, P. M. Viruela, E. Orti, K. Takimiya and T. Otsubo, *Angew. Chem., Int. Ed.*, 2007, **46**, 9057–9061.
86 J. Casado and J. T. López Navarrete, *Chem. Rec.*, 2011, **11**, 45–53.
87 V. Hernández, J. Casado, F. J. Ramírez, G. Zotti, S. Hotta and J. T. López Navarrete, *J. Chem. Phys.*, 1996, **104**, 9271.
88 J. Casado, V. Hernández, S. Hotta and J. T. López Navarrete, *J. Chem. Phys.*, 1998, **109**, 10419.
89 D. Fazzi, E. V. Canesi, F. Negri, C. Bertarelli and C. Castiglioni, *ChemPhysChem*, 2010, **11**, 3685–3695.
90 S. Di Motta, F. Negri, D. Fazzi, C. Castiglioni and E. V. Canesi, *J. Phys. Chem. Lett.*, 2010, **1**, 3334–3339.
91 S. R. González, Y. Ie, Y. Aso, J. T. López Navarrete and J. Casado, *J. Am. Chem. Soc.*, 2011, **133**, 16350–16353.
92 T. Nishinaga, M. Tateno, M. Fujii, W. Fujita, M. Takase and M. Iyoda, *Org. Lett.*, 2010, **12**, 5374–5377.

